



6-2021

## Outcomes of Aspheric Primaries in Robe's Circular Restricted Three-body Problem

Bhavneet Kaur  
*University of Delhi*

Shipra Chauhan  
*University of Delhi*

Dinesh Kumar  
*University of Delhi*

Follow this and additional works at: <https://digitalcommons.pvamu.edu/aam>

 Part of the [Dynamic Systems Commons](#)

### Recommended Citation

Kaur, Bhavneet; Chauhan, Shipra; and Kumar, Dinesh (2021). Outcomes of Aspheric Primaries in Robe's Circular Restricted Three-body Problem, *Applications and Applied Mathematics: An International Journal (AAM)*, Vol. 16, Iss. 1, Article 25.

Available at: <https://digitalcommons.pvamu.edu/aam/vol16/iss1/25>

This Article is brought to you for free and open access by Digital Commons @PVAMU. It has been accepted for inclusion in *Applications and Applied Mathematics: An International Journal (AAM)* by an authorized editor of Digital Commons @PVAMU. For more information, please contact [hvkoshy@pvamu.edu](mailto:hvkoshy@pvamu.edu).



## Outcomes of Aspheric Primaries in Robe's Circular Restricted Three-body Problem

<sup>1</sup>Bhavneet Kaur, <sup>2\*</sup>Shipra Chauhan and <sup>3</sup>Dinesh Kumar

<sup>1</sup>Department of Mathematics  
Lady Shri Ram College for Women  
University of Delhi  
Delhi, India  
[bhavneet.lsr@gmail.com](mailto:bhavneet.lsr@gmail.com)

<sup>2,3</sup>Department of Mathematics  
Deshbandhu College  
University of Delhi  
Delhi, India  
<sup>2</sup>[chauhanshipra10@gmail.com](mailto:chauhanshipra10@gmail.com);  
<sup>3</sup>[dineshk8392@gmail.com](mailto:dineshk8392@gmail.com)

\*Corresponding Author

Received: September 16, 2020; Accepted: January 17, 2021

### Abstract

We consider the Robe's restricted three-body problem in which the bigger primary is assumed to be a hydrostatic equilibrium figure as an oblate spheroid filled with a homogeneous incompressible fluid, around which a circular motion is described by the second primary, that is a finite straight segment. The aim of this note is to investigate the effect of oblateness and length parameters on the motion of an infinitesimal body that lies inside the bigger primary. The locations of the equilibrium points are approximated by the series expansions and it is found that two collinear equilibrium points lying on the line segment joining the centers of the primaries, exist. The non-collinear equilibrium points lie on a circle and are infinite in number. No out-of-plane equilibrium point exists. Based on the linear stability analysis, it is observed that the collinear equilibrium points can be stable under certain conditions whereas the non-collinear ones are always unstable.

**Keywords:** Robe's circular restricted three-body problem; Oblate spheroid; Finite straight segment; Equilibrium points

**MSC 2010 No.:** 37N05, 70F07, 70F15

## 1. Introduction

Robe, in 1977, contemplated a new kind of restricted three-body problem, considering the bigger primary as a rigid spherical shell filled with a homogenous incompressible fluid of density  $\rho_1$ , and the smaller primary is considered to be a point mass, that lies outside the bigger primary. He analysed the motion of an infinitesimal body which is considered to be a small solid sphere of density  $\rho_3$ , that moves inside the bigger primary, under the influence of buoyancy force of the fluid and attraction of the smaller primary. An equilibrium point at the center of the bigger primary was found, and he discussed its linear stability for the circular and elliptical cases.

The origin of such three-body problems can be traced back to Robe's work, that proved out to be pivot point for further studies of finding equilibrium points and their stability under many perturbing forces like oblateness and triaxiality, done by many researchers in the following years.

The study of effects of perturbation on the location of equilibrium points in the Robe's model (1977) for the circular case was carried out by Shrivastava and Garain in 1991. For the case when  $\rho_1 = \rho_3$ , they noticed that there is only one equilibrium point certainly affected by the perturbation, which lies between the origin and the center of the bigger primary. Both Robe (1977) and Shrivastava and Garain (1991) assumed that the pressure field of the fluid  $\rho_1$  has spherical symmetry around the center of the shell. They considered only one of the three components of the pressure field, that is due to its own gravitational field of the fluid  $\rho_1$ .

The other two remaining components that are originating in the attraction of  $m_2$  and arising from the centrifugal force were taken into account by Plastino and Plastino in 1995. They revisited the Robe's problem by assuming the hydrostatic equilibrium figure of the bigger primary as Roche's ellipsoid. In addition, they tentatively stated that the effect of buoyancy forces might be thought as equivalent to a perturbation of the Coriolis force.

Hallan and Rana (2001) investigated the equilibrium points in the Robe's circular restricted three-body problem, in which there are two collinear and infinite number of non-collinear equilibrium points, for certain values of mass and density parameters. They also studied the stability of all the equilibrium points obtained for the problem.

The positions and linear stability of an infinitesimal body around the equilibrium points in the framework of Robe's restricted three-body problem, with the assumption that the bigger primary is an oblate spheroid have been studied by Hallan and Mangang in 2007. They pointed out the oblateness effect on the positions of the equilibrium points. Under certain conditions, two collinear equilibrium points, lying on the line segment joining the centers of the primaries, and infinite number of non-collinear points exist. By the stability analysis, it has been deduced that the collinear equilibrium points are conditionally stable, whereas non-collinear ones are always unstable.

In addition to the framework of Hallan and Mangang (2007), Singh and Mohammed in 2012 assumed the shape of smaller primary as a triaxial rigid body. A collinear equilibrium point is found near the center of the first primary which is conditionally stable. The points lying on the ellipse and

inside the bigger primary are called elliptical points by them, and they also pointed out the effect of oblateness and triaxiality on these points which are infinite in number.

In 2012, Singh and Sandah worked on Robe's circular restricted three-body problem, with both primaries as oblate bodies. Singh and Mohammed in 2012 considered the problem by taking primaries as oblate and triaxial bodies each, which can be seen as an extension of Hallan and Mangang (2007). They performed stability analysis of collinear and elliptical points. Out-of-plane equilibrium points and their stability have been checked by them in 2013.

In 2001, Riaguas et al. studied the linear and non-linear stability of the equilibrium points in the restricted three-body problem, with one body being taken as finite straight segment. Jain and Sinha (2014b) studied the linear stability of equilibrium points and the regions of motion in the restricted three-body problem, with both the primaries taken as finite straight segments. Also, Jain and Sinha (2014a) discussed the non-linear stability of non-collinear equilibrium points with one primary as finite segment under the resonance. Chauhan et al. (2018) examined the restricted three-body problem under the effect of albedo with the smaller primary being a finite straight segment.

Recently Kumar et al. (2019) studied the Robe's restricted three-body problem that comprises of the smaller primary as a finite straight segment. The two collinear equilibrium points are found, that are conditionally stable. Infinite non-collinear equilibrium points and two out-of-plane equilibrium points are always unstable. Furthermore, the effect of viscosity in Robe's circular restricted three-body problem has been examined by Ansari et al. (2019) and Kaur et al. (2020b).

Many research works were undertaken in the restricted problem of  $2 + 2$  bodies. The problem of Robe's restricted three-body was extended to the problem of  $2 + 2$  bodies by Kaur and Aggarwal (2012), in which the mutually attracting infinitesimal bodies were taken as small solid spheres. The Robe's restricted problem of  $2 + 2$  bodies where the bigger primary is a Roche ellipsoid has also been studied by Kaur and Aggarwal (2013a). Later, Kaur and Aggarwal (2013b) and Aggarwal and Kaur (2014) studied the Robe's restricted problem of  $2 + 2$  bodies, when one of the primaries is an oblate body.

We modify the model of Robe's by considering the hydrostatic equilibrium figure (Chandrashekhara (1987)) of the fluid  $\rho_1$  as an oblate spheroid and smaller one as a finite straight segment. Our main focus of the study is to determine the influences on the positions and stability of equilibrium points of a small solid sphere  $m_3$  of density  $\rho_3$  moving inside  $m_1$ , caused by the oblateness  $A$  of  $m_1$  and length  $l$  of  $m_2$ . We have discussed the case of unequal densities, that is when  $\rho_1 \neq \rho_3$ . For the sake of completeness a particular case of equal densities is also presented as discussed by Robe (1977) and Shrivastava and Garain (1991).

This paper is divided in the following sections. Section 1 includes the development of the problem over the years. In Section 2, the problem has been stated and the equations of motion of  $m_3$  are derived following the methodology as in Plastino and Plastino (1995) and Kumar et al. (2019), with a separate subsection of mean motion that is obtained by using the necessary expression from Brouwer and Clemence (1961). In Section 3, collinear and non-collinear equilibrium points are calculated for the two cases when  $\rho_1 = \rho_3$  and  $\rho_1 \neq \rho_3$  under the influences of  $A$  and  $l$ . Linear

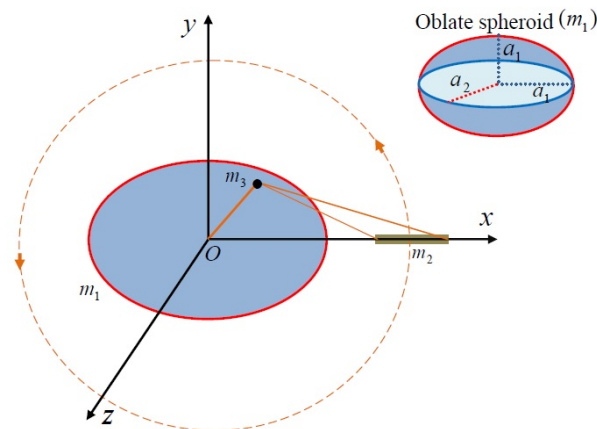


**Figure 1.** The Robe's circular restricted three-body problem in a synodic reference frame with  $m_1$  as an oblate spheroid and  $m_2$  a finite straight segment

stability analysis of the obtained equilibrium points has been performed in Section 4 by using the characteristic equations. Section 5 includes the application of the work presented in the present manuscript. Sections 6 and 7 provide a brief resume of the work carried out in this paper.

## 2. Equations of Motion

To begin with, we assume that the bigger primary of mass  $m_1$  is described by an oblate spheroid filled with a homogeneous incompressible fluid of density  $\rho_1$ . The smaller primary of mass  $m_2$  ( $< m_1$ ) lying outside  $m_1$  assumes the shape of a finite straight segment of length  $2l'$  and moves in a circular orbit with angular velocity  $\omega$  around  $m_1$ . The infinitesimal mass  $m_3$  ( $\ll m_2$ ) having density  $\rho_3$  moves inside  $m_1$ . We adopt a coordinate system  $Oxyz$  with the origin at the center of mass  $O$  of  $m_1$ ,  $Ox$  pointing towards  $m_2$  and  $Oxy$  being the orbital plane of  $m_2$  as shown in Figure 1.

Let the synodic coordinate system initially coincident with the inertial system (coincident in the sense that the respective  $x$ -axes of the two systems overlap each other and the other axes are parallel) that rotate with the same angular velocity  $\omega$  of  $m_2$ . We assume that the principal axes of  $m_2$  is parallel to the synodic axes and their axes of symmetry be perpendicular to the plane of motion of the bodies.

The various forces per unit mass acting on  $m_3$  are

- The gravitational force exerted by the finite straight segment of mass  $m_2$  on  $m_3$ ;
- The buoyancy force acting on  $m_3$  arising in the fluid;
- The attraction of the fluid of density  $\rho_1$ .

Now, to make the system dimensionless, we take the unit of mass, and distance is such that the sum of the masses of the primaries is 1 unit, and distance between the primaries is also 1 unit, that is  $R = 1$ . We choose the unit of time such that  $G$  becomes unity. According to these choices of

units, the equations of motion of  $m_3$  in the dimensionless variables are given by

$$\ddot{x} - 2\omega\dot{y} = \Omega_x, \quad (1a)$$

$$\ddot{y} + 2\omega\dot{x} = \Omega_y, \quad (1b)$$

$$\ddot{z} = \Omega_z, \quad (1c)$$

where

$$\Omega = \rho \left[ \pi \rho_1 (I - A_1 x^2 - A_1 y^2 - A_2 z^2) + \frac{1}{2} \omega^2 ((x - \mu)^2 + y^2) + \frac{\mu}{2l} \log \left( \frac{r_1 + r_2 + 2l}{r_1 + r_2 - 2l} \right) \right],$$

$$l = \frac{l'}{R}, \quad A = \frac{a_1^2 - a_2^2}{5R^2}, \quad 0 < l \ll 1, \quad 0 < A \ll 1,$$

$$\mu = \frac{m_2}{m_1 + m_2}, \quad 0 < \mu < 1, \quad \rho = 1 - \frac{\rho_1}{\rho_3},$$

$$r_1^2 = (x - 1 + l)^2 + y^2 + z^2, \quad r_2^2 = (x - 1 - l)^2 + y^2 + z^2,$$

$$A_1 = a_1^2 a_2 \int_0^\infty \frac{du}{\Delta (a_1^2 + u)}, \quad A_2 = a_1^2 a_2 \int_0^\infty \frac{du}{\Delta (a_2^2 + u)},$$

$$I = 2a_1^2 A_1 + a_2^2 A_2, \quad \Delta^2 = (a_1^2 + u)^2 (a_2^2 + u).$$

Here,  $a_1$  and  $a_2$  are the equatorial and polar radii of the bigger primary;  $\Omega_x, \Omega_y$  and  $\Omega_z$  are the partial derivatives of  $\Omega$  with respect to  $x, y$  and  $z$ , respectively, and dot signifies the differentiation with respect to time in dimensionless variables.

Equations (1a)-(1c) are the equations of motion of  $m_3$  of our problem under the influence of the buoyancy force of the fluid, oblateness of  $m_1$  and the gravitational attractions of  $m_1$  and  $m_2$ . These obtained equations are analogous to the equations as in Hallan and Mangang (2007) on taking the length parameter  $l = 0$ . The equations of motion of Kumar et al. (2019) can be obtained from Equations (1a)-(1c) by taking the center of  $m_1$  at  $(-\mu, 0, 0)$  and neglecting the effect of oblateness  $A$ .

## 2.1. Mean motion of the primaries

Let us consider the gravitational potential between two finite bodies of masses  $m_1$  and  $m_2$  be given by

$$V^* = \frac{Gm_1 m_2}{R} + \frac{Gm_2}{2R^3} (A_{11} + A_{12} + A_{13} - 3I_1) + \frac{Gm_1}{2R^3} (A_{21} + A_{22} + A_{23} - 3I_2), \quad (2)$$

where  $G$  is constant of gravitation;  $m_1, m_2$  are the masses of the bigger and smaller primary, respectively;  $R$  is the distance between the primaries;  $A_{11}, A_{12}, A_{13}$  are the moment of inertia of  $m_1$  about the principal axes;  $A_{21}, A_{22}, A_{23}$  are the moment of inertia of  $m_2$  about the principal axes;  $I_1$  and  $I_2$  are the moment of inertia of  $m_1$  and  $m_2$  respectively about the line joining the center of mass of the primaries.

Since the center of mass of the primaries lie on the  $x$ -axis, therefore,  $I_1 = A_{11}$  and  $I_2 = A_{21}$ . In

the present problem  $m_1$  is an oblate spheroid and  $m_2$  a finite straight segment, therefore,

$$A_{11} = A_{12} = \frac{m_1(a_1^2 + a_2^2)}{5}, A_{13} = \frac{2}{5}m_1a_1^2, A_{21} = 0, A_{22} = A_{23} = \frac{1}{3}m_2l'^2.$$

Therefore, Equation (2) reduces into the following form,

$$V^* = Gm_1m_2 \left( \frac{1}{R} + \frac{a_1^2 - a_2^2}{10R^3} + \frac{l'^2}{3R^3} \right).$$

Thus, the gravitational force between  $m_1$  and  $m_2$  is

$$F_1 = - \frac{\partial V^*}{\partial R} = Gm_1m_2 \left( \frac{1}{R^2} + \frac{3(a_1^2 - a_2^2)}{10R^4} + \frac{l'^2}{R^4} \right).$$

Since  $m_2$  is moving in circular orbit around  $m_1$ , therefore,

$$\omega^2 R = G(m_1 + m_2) \left( \frac{1}{R^2} + \frac{3(a_1^2 - a_2^2)}{10R^4} + \frac{l'^2}{R^4} \right).$$

Using dimensionless variables, we have

$$\omega^2 = 1 + \frac{3}{2}A + l^2.$$

It is observed that, the mean motion is affected by the oblateness and length parameters. A comparative study of mean motion is as follows.

- If smaller primary is considered as a point mass, that is,  $l = 0$ , mean motion agree with Sharma and Subbarao (1976), Hallan and Mangang (2007), and Wang et al. (2018).
- If oblateness of bigger primary is neglected, that is,  $A = 0$ , mean motion becomes similar to Kaur et al. (2020a).

### 3. Equilibrium Points

The points where the infinitesimal mass has zero velocity and zero acceleration in the rotating frame are known as equilibrium points. By equilibrium point, we mean a point  $(x, y, z)$  in the rotating frame, such that

$$\Omega_x(x, y, z) = 0, \Omega_y(x, y, z) = 0 \text{ and } \Omega_z(x, y, z) = 0.$$

That is, the locations of equilibrium points are obtained by solving

$$\rho \left[ \omega^2(x - \mu) - 2\pi\rho_1 A_1 x - \frac{2\mu}{[(r_1 + r_2)^2 - 4l^2]} \left( \frac{x - 1 + l}{r_1} + \frac{x - 1 - l}{r_2} \right) \right] = 0, \quad (3a)$$

$$\rho \left[ \omega^2 - 2\pi\rho_1 A_1 - \frac{2\mu(r_1 + r_2)}{r_1 r_2 [(r_1 + r_2)^2 - 4l^2]} \right] y = 0, \quad (3b)$$

$$\rho \left[ 2\pi\rho_1 A_2 + \frac{2\mu(r_1 + r_2)}{r_1 r_2 [(r_1 + r_2)^2 - 4l^2]} \right] z = 0, \quad (3c)$$

simultaneously.

For the particular case when the infinitesimal body has the same density as that of the fluid, that is  $\rho_1 = \rho_3$ , it is indistinguishable from any of the fluid's elements. On solving Equations (1a)-(1c), we have

$$\begin{aligned}x &= C_1 \cos(2\omega t + \tau) + C_2, \\y &= -C_1 \sin(2\omega t + \tau) + C_3, \\z &= C_4 t + C_5,\end{aligned}$$

where  $C_1, C_2, C_3, C_4, C_5$  and  $\tau$  are the constants of integration. Therefore, all triplets  $(x, y, z)$  are the equilibrium points since the fluid is assumed to be in hydrostatic equilibrium in the rotating frame.

Next, we find the equilibrium points when the infinitesimal body is denser than the fluid, that is  $\rho_3 > \rho_1$ , consequently  $\rho > 0$ . From Equation (3c), we observe that either  $z = 0$ , or

$$2\pi\rho_1 A_2 + \frac{2\mu(r_1 + r_2)}{r_1 r_2 [(r_1 + r_2)^2 - 4l^2]} = 0.$$

The second equation is not possible, therefore  $z = 0$ . The equilibrium points lie in the plane of motion of the primaries, when the infinitesimal body is denser than the fluid ( $\rho > 0$ ). Therefore, the motion of  $m_3$  is possible only in  $xy$ -plane.

### 3.1. Collinear equilibrium points

The points lying on the  $x$ -axis are collinear equilibrium points. These are obtained from Equations (3a) and (3b) by taking  $y = z = 0$ . Therefore, they are of the form  $(x, 0, 0)$ , where the  $x$ -coordinates are the solutions of the equation

$$\omega^2(x - \mu) - 2\pi\rho_1 A_1 x - \frac{2\mu}{[(r_1 + r_2)^2 - 4l^2]} \left( \frac{x - 1 + l}{r_1} + \frac{x - 1 - l}{r_2} \right) = 0,$$

where  $r_1 = |x - 1 + l|$  and  $r_2 = |x - 1 - l|$ . Since  $m_3$  lies inside  $m_1$  and the circular motion of  $m_2$  is described around  $m_1$ , therefore,  $x < 1 - l$ . On simplifying the above equation, we obtain the following expression

$$\left( 1 + l^2 + \frac{3}{2}A \right) (x - \mu) - 2\pi\rho_1 A_1 x - \frac{\mu}{[l^2 - (x - 1)^2]} = 0. \quad (4)$$

In the absence of oblateness and length parameters  $A$  and  $l$ , respectively, Equation (4) takes the following form

$$x \left[ (1 - 2\pi\rho_1 A_1)x^2 + (-2 - \mu + 4\pi\rho_1 A_1)x + (1 + 2\mu - 2\pi\rho_1 A_1) \right] = 0. \quad (5)$$

It can be seen that the center of the bigger primary is an equilibrium point for all the parameters involved since  $x = 0$  is a trivial solution of Equation (5). The other non-trivial solution of Equation (5) lying inside  $m_1$  is

$$x_1 = 1 + \frac{\mu + \sqrt{\mu^2 + 8\pi\rho_1 A_1 \mu - 4\mu}}{2(1 - 2\pi\rho_1 A_1)},$$

provided  $1 - 2\pi\rho_1 A_1 + \frac{3}{4}\mu < 0$  and  $|x_1| < a_1$ .

**Table 1.** The locations of  $L_1$  and  $L_2$  for the different values of  $A$

$\mu$	$l$	$A_1$	$\rho_1$	$A$	$L_1(x, 0, 0)$	$L_2(x', 0, 0)$
0.1	0.0001	0.3	0.649	$10^{-6}$	$(-6.42767 \times 10^{-6}, 0, 0)$	$(0.0705201, 0, 0)$
0.1	0.0001	0.3	0.649	0.004	$(-0.00245286, 0, 0)$	$(0.0757452, 0, 0)$
0.1	0.0001	0.3	0.649	0.01	$(-0.06000460, 0, 0)$	$(0.0803995, 0, 0)$
0.1	0.0001	0.3	0.649	0.02	$(-0.12156500, 0, 0)$	$(0.0848725, 0, 0)$
0.1	0.0001	0.3	0.649	0.04	$(-0.26846000, 0, 0)$	$(0.0894293, 0, 0)$

Next, we find the roots of Equation (4) when the oblateness and length parameters  $A$  and  $l$  of  $m_1$  and  $m_2$  respectively, are considered to be non-zero. Let the roots of Equation (4) for this case be

$$x = 0 + p_1 \text{ and } x = x_1 + p_2 \text{ with } |p_i| \ll 1, i = 1, 2,$$

where the expressions for  $p_1$  and  $p_2$  are given by Equation (6) and are obtained by putting the above values in Equation (4) with the first order terms of  $p_1, p_2, A$  and up to second order terms of  $l$

$$p_1 = \frac{3}{2} \left[ \frac{A\mu}{1 + 2\mu - 2\pi\rho_1 A_1} \right],$$

$$p_2 = \frac{-\mu l^2 (1 - x_1)^{-3} + (x_1 - \mu)(x_1 - 1)(l^2 + \frac{3}{2}A)}{2\mu + (1 - 2\pi\rho_1 A_1)(1 - 3x_1)}. \quad (6)$$

Therefore, on taking the effects of oblateness and length parameter into consideration,  $L_1(p_1, 0, 0)$  and  $L_2(x_1 + p_2, 0, 0)$  are the equilibrium points near the center of the bigger primary.  $L_2$  exists provided  $1 - 2\pi\rho_1 A_1 < -\frac{3\mu}{4}$  and  $|x_1| < a_1$ .

**Table 2.** The locations of  $L_2$  for the different values of  $l$

$\mu$	$A$	$A_1$	$\rho_1$	$l$	$L_2(x', 0, 0)$
0.1	0.0001	0.3	0.649	0.0001	$(0.0706889, 0, 0)$
0.1	0.0001	0.3	0.649	0.05	$(0.0605384, 0, 0)$
0.1	0.0001	0.3	0.649	0.07	$(0.0506251, 0, 0)$
0.1	0.0001	0.3	0.649	0.08	$(0.0443311, 0, 0)$
0.1	0.0001	0.3	0.649	0.09	$(0.0370857, 0, 0)$

For the notational convenience, we write  $x' = x_1 + p_2$ . The coordinates of collinear equilibrium points  $L_1$  and  $L_2$  for the different values of oblateness parameter  $A$  and the fixed values of  $\mu, l, A_1$  and  $\rho_1$  are given in Table 1. From Figure 2, it is noticeable that increase in the effect of oblateness parameter  $A$  results in the collinear equilibrium point  $L_2$  moving towards the center of  $m_2$  and away from the center of  $m_1$ . However,  $L_1$  drifts away from the center of  $m_1$  in its left direction.

From the expressions of  $p_1$  and  $p_2$ , it is clearly seen that the length of  $m_2$  has a substantial effect on the position of  $L_2$ , and zero effect on  $L_1$ . In Table 2, the effect of  $l$  is observed for the fixed values of  $\mu, A, A_1$  and  $\rho_1$ , and varying values of  $l$ . The point  $L_2$  shifts towards the center of the bigger primary with the increasing values of  $l$ . This effect is shown pictorially in Figure 3. As the mass

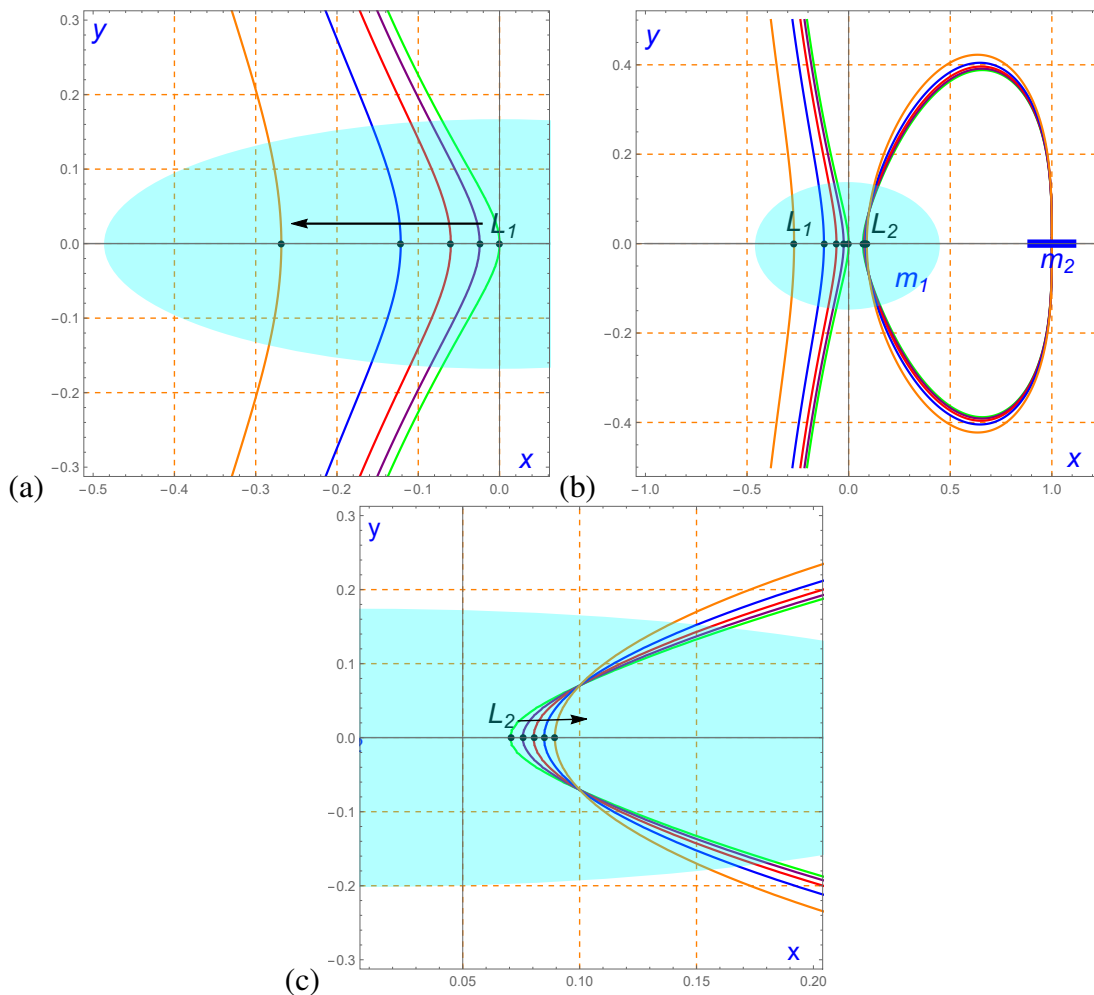


**Figure 2.** The locations of  $L_1$  and  $L_2$  for  $\mu = 0.1$ ,  $l = 0.0001$ ,  $A_1 = 0.3$ ,  $\rho_1 = 0.649$  and different values of oblateness parameter  $A = 10^{-6}$  (green), 0.004 (purple), 0.01 (red), 0.02 (blue), 0.04 (orange). The black dots represent the positions of  $L_1$  and  $L_2$ , that are shown in (b). The zoomed portions of the positions of  $L_1$  and  $L_2$  are shown in (a) and (c), respectively.

parameter  $\mu$  increases from 0.1 to 0.2, the abscissas of  $L_1$  and  $L_2$  decrease for the fixed values of  $A$ ,  $A_1$ ,  $\rho_1$  and  $l$ . Numerically this effect is computed in Table 3 and depicted in Figure 4.

**Table 3.** The locations of  $L_1$  and  $L_2$  for the different values of  $\mu$

$A$	$A_1$	$\rho_1$	$l$	$\mu$	$L_1(p_1, 0, 0)$	$L_2(x', 0, 0)$
0.0001	0.3	0.649	0.0001	0.10	(-0.0006416, 0, 0)	(0.070688900, 0, 0)
0.0001	0.3	0.649	0.0001	0.12	(-0.0509388, 0, 0)	(0.001047040, 0, 0)
0.0001	0.3	0.649	0.0001	0.15	(-0.2224320, 0, 0)	(0.000292415, 0, 0)
0.0001	0.3	0.649	0.0001	0.18	(-0.3879910, 0, 0)	(0.000197195, 0, 0)
0.0001	0.3	0.649	0.0001	0.20	(-0.4956600, 0, 0)	(0.000169572, 0, 0)

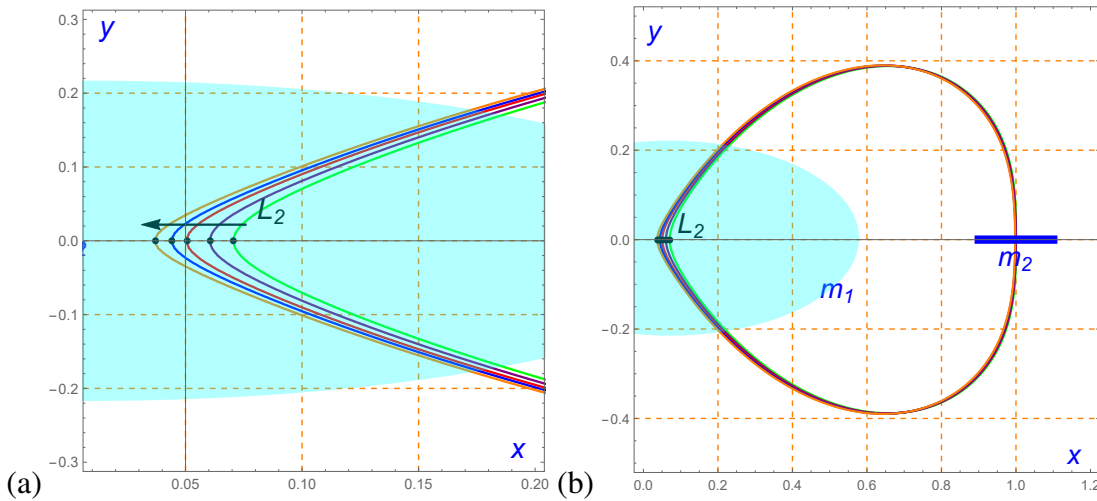


**Figure 3.** The locations of  $L_2$  for  $\mu = 0.1$ ,  $A = 0.0001$ ,  $A_1 = 0.3$ ,  $\rho_1 = 0.649$  and different values of the length parameter  $l = 0.0001$  (green),  $0.05$  (purple),  $0.07$  (red),  $0.08$  (blue),  $0.09$  (orange). The black dots represent the position of  $L_2$ , that are shown in (b). The zoomed portion of the positions of  $L_2$  is shown in (a).

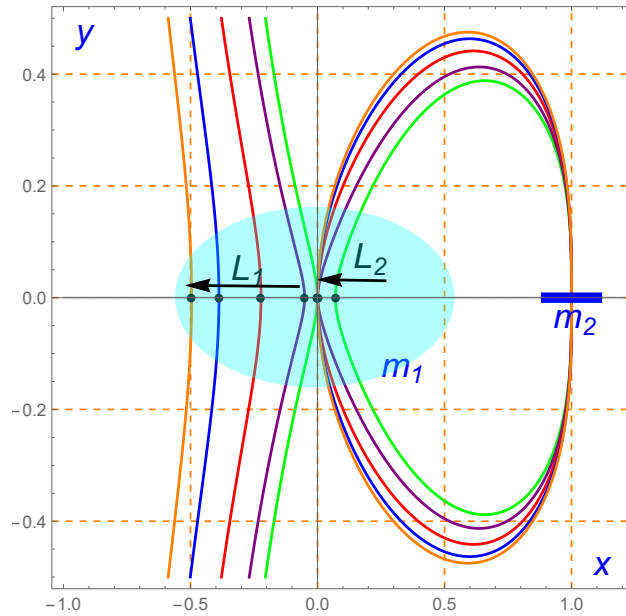


**Figure 4.** The locations of  $L_1$  and  $L_2$  for  $A = 0.0001$ ,  $A_1 = 0.3$ ,  $\rho_1 = 0.649$ ,  $l = 0.0001$  and different values of the mass parameter  $\mu = 0.1$  (green),  $0.12$  (purple),  $0.15$  (red),  $0.18$  (blue),  $0.2$  (orange). The black dots represent the collinear equilibrium points  $L_1$  and  $L_2$ .

### 3.2. Non-collinear equilibrium points

The locations of non-collinear equilibrium points are evaluated by taking  $x \neq 0$ ,  $y \neq 0$  and  $z = 0$  in Equations (3a) and (3b). These are the solutions of equations:

$$\omega^2(x - \mu) - \frac{2\mu}{[(r_1 + r_2)^2 - 4l^2]} \left( \frac{x - 1 + l}{r_1} + \frac{x - 1 - l}{r_2} \right) - 2\pi\rho_1 A_1 x = 0, \tag{7a}$$

$$\omega^2 - \frac{2\mu}{[(r_1 + r_2)^2 - 4l^2]} \left( \frac{1}{r_1} + \frac{1}{r_2} \right) - 2\pi\rho_1 A_1 = 0. \tag{7b}$$

On solving Equations (7a) and (7b) by retaining the terms up to first and second order of the oblateness and length parameters  $A$  and  $l$ , respectively, we have

$$(1 - x)^2 + y^2 = 1 - \left( A + \frac{2}{3}l^2 \right). \tag{8}$$

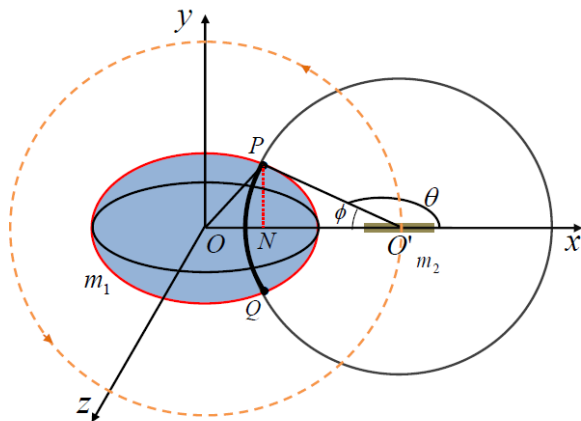


**Figure 5.** The points on the arc  $PQ$  lying inside  $m_1$  show the position of non-collinear equilibrium points.

The points on the above circle lying within the first primary  $m_1$  are the non-collinear equilibrium (or circular) points as shown in Figure 5, provided

$$2\pi\rho_1A_1 = (1 - \mu) \left( 1 + l^2 + \frac{3}{2}A \right).$$

The positions of circular points are affected by the oblateness and length parameters. This fact differentiates our results from Kumar et al. (2019), in which the position of circular points are affected by the length parameter  $l$  of  $m_2$  only.

#### 4. Stability Analysis

Just knowing the numbers of equilibrium points for a dynamical system is not sufficient – we also need to determine the stability of these points. In this section, we will find the domain of linear stability for the parameters characterizing the problem. To perform such analysis, let the third body be displaced to  $(x_0 + \xi, y_0 + \eta, z_0 + \zeta)$  from the equilibrium point  $(x_0, y_0, z_0)$  where  $(\xi, \eta, \zeta)$  is a small displacement. Expanding the equations of motion (3a)–(3c) up to first order terms with respect to  $\xi, \eta$  and  $\zeta$ , we get the variational equations

$$\ddot{\xi} - 2\omega\dot{\eta} = \Omega_{xx}^0\xi + \Omega_{xy}^0\eta + \Omega_{xz}^0\zeta, \tag{9a}$$

$$\ddot{\eta} + 2\omega\dot{\xi} = \Omega_{yx}^0\xi + \Omega_{yy}^0\eta + \Omega_{yz}^0\zeta, \tag{9b}$$

$$\ddot{\zeta} = \Omega_{zx}^0\xi + \Omega_{zy}^0\eta + \Omega_{zz}^0\zeta, \tag{9c}$$

where the superscript “0” denotes that the second order derivatives being evaluated at the point  $(x_0, y_0, z_0)$ .

#### 4.1. Stability of the collinear equilibrium point $L_1$

At the collinear equilibrium point  $L_1$ , the values of second order partial derivatives of  $\Omega$  are

$$\begin{aligned}\Omega_{xx}^0 &= \frac{3\rho\mu A}{2p_1} = a_{11}, \quad \Omega_{yy}^0 = 3\rho\mu \left( \frac{A}{2p_1} - 1 \right) = a_{22}, \\ \Omega_{zz}^0 &= -\rho (2\pi\rho_1 A_2 + \mu(1 + 3p_1 + 2\mu l^2)) = a_{33}, \\ \Omega_{yz}^0 &= 0, \quad \Omega_{xy}^0 = 0 \text{ and } \Omega_{xz}^0 = 0.\end{aligned}$$

The variational Equations (9a)-(9c) become

$$\ddot{\xi} - 2\omega\dot{\eta} = a_{11}\xi, \quad (10a)$$

$$\dot{\eta} + 2\omega\dot{\xi} = a_{22}\eta, \quad (10b)$$

$$\ddot{\zeta} = a_{33}\zeta. \quad (10c)$$

The motion of the infinitesimal mass along  $z$ -axis is stable since the solution of Equation (10c) is bounded. Let the Equations (10a) and (10b) has solutions of the form

$$\xi = B_1 e^{\lambda t} \text{ and } \eta = B_2 e^{\lambda t},$$

where  $B_1, B_2$  are the arbitrary constants. On substituting these values in Equations (10a) and (10b), we obtain

$$\begin{bmatrix} \lambda^2 - a_{11} & -2\omega\lambda \\ -2\omega\lambda & a_{22} - \lambda^2 \end{bmatrix} \begin{bmatrix} B_1 \\ B_2 \end{bmatrix} = \begin{bmatrix} 0 \\ 0 \end{bmatrix}.$$

For the non-trivial solution, we must have

$$\begin{vmatrix} \lambda^2 - a_{11} & -2\omega\lambda \\ -2\omega\lambda & a_{22} - \lambda^2 \end{vmatrix} = 0,$$

equivalently

$$\lambda^4 - v_1\lambda^2 + v_2 = 0, \quad (11)$$

where  $v_1 = a_{11} + a_{22} - 4\omega^2$  and  $v_2 = a_{11}a_{22}$ . Equation (11) can be converted in to the following quadratic equation by taking  $\lambda^2 = \Lambda$ ,

$$\Lambda^2 - v_1\Lambda + v_2 = 0.$$

The equilibrium point is stable if  $v_1 < 0$  and  $v_2 > 0$ . We observe the following:

- If  $p_1 < 0$ , then  $a_{11} < 0$  and  $a_{22} < 0$ , therefore,  $L_1$  is stable.
- If  $0 < p_1 < A/2$ , then  $a_{11} > 0$  and  $a_{22} > 0$ . For this case  $v_2 > 0$ . Further, if  $v_1 < 0$ , then  $L_1$  is stable.
- If  $0 < (A/2) < p_1$ , then  $a_{11} > 0$  and  $a_{22} < 0$ . Therefore,  $L_1$  is unstable.

### 4.2. Stability of the collinear equilibrium point $L_2$

For the collinear equilibrium point  $L_2$ , we have

$$\begin{aligned} \Omega_{xx}^0 &= \rho \left[ 1 - 2\pi\rho_1 A_1 - \frac{2\mu}{(1-x')^3} + \frac{3A}{2} + \left( 1 - \frac{4\mu}{(1-x')^5} \right) l^2 \right] = a'_{11}, \\ \Omega_{yy}^0 &= \rho \left[ 1 - 2\pi\rho_1 A_1 - \frac{\mu}{(1-x')^3} + \frac{3A}{2} + \left( 1 - \frac{2\mu}{(1-x')^5} \right) l^2 \right] = a'_{22}, \\ \Omega_{zz}^0 &= -\rho \left[ 2\pi\rho_1 A_2 + \frac{\mu}{(1-x')^3} + \frac{2\mu l^2}{(1-x')^5} \right] = a'_{33}, \\ \Omega_{xy}^0 &= 0, \quad \Omega_{xz}^0 = 0 \text{ and } \Omega_{yz}^0 = 0. \end{aligned}$$

The corresponding variational equations (9a)-(9c) are

$$\ddot{\xi} - 2\omega\dot{\eta} = a'_{11}\xi, \tag{12a}$$

$$\ddot{\eta} + 2\omega\dot{\xi} = a'_{22}\eta, \tag{12b}$$

$$\ddot{\zeta} = a'_{33}\zeta. \tag{12c}$$

The motion of the infinitesimal mass along  $z$ -axis is stable since the solution of Equation (12c) is bounded. The characteristic equation of Equations (12a) and (12b) is

$$\lambda^4 - v'_1\lambda^2 + v'_2 = 0$$

where  $v'_1 = a'_{11} + a'_{22} - 4\omega^2$  and  $v'_2 = a'_{11}a'_{22}$ . The point  $x' < 0$  if  $x_1 < 0$  since  $|p_2| \ll 1$ . The equilibrium point  $L_2$  is stable because  $v'_1 < 0$  and  $v'_2 > 0$ . Also for the case when  $x' > 0$ , the equilibrium point is stable if the above two conditions are satisfied.

### 4.3. Stability of the non-collinear equilibrium points

As calculated earlier, the non-collinear equilibrium points lie on the circle given by Equation (8) exist only when  $2\pi\rho_1 A_1 = (1 - \mu) \left( 1 + l^2 + \frac{3}{2}A \right)$ . The general coordinate of a circular point are of the form  $(1 + r \cos \theta, r \sin \theta, 0)$  with the parameter  $\theta$ . From Figure 5, we have

$$\begin{aligned} 180^\circ - \phi &\leq \theta \leq 180^\circ + \phi, \\ \text{where } \phi &= \sin^{-1} \left( \frac{PN}{O'P} \right). \end{aligned}$$

Here  $PN = 2\sqrt{s(s-OP)(s-O'P)(s-1)}$  with  $s = \frac{OP+O'P+1}{2}$ ,  $OP$  is the radius of  $m_1$  and  $O'P$  is the radius of the circle given by Equation (8). At circular points, the values of second order

partial derivatives are

$$\Omega_{xx}^0 = \rho\mu \left[ 3 \left( 1 + \frac{3}{2}A \right) \cos^2 \theta + \left( \frac{3}{2} - 12 \cos^2 \theta + \frac{35}{2} \cos^4 \theta \right) l^2 \right] = a_{11}^0,$$

$$\Omega_{yy}^0 = \rho\mu \left[ 3 \left( 1 + \frac{3}{2}A \right) \sin^2 \theta + \frac{1}{2} (1 - 5 \cos^2 \theta + \sin^2 \theta + 35 \cos^2 \theta \sin^2 \theta) l^2 \right] = a_{22}^0,$$

$$\Omega_{xy}^0 = \rho\mu \left[ 3 \left( 1 + \frac{3}{2}A \right) + \frac{1}{2} (-9 + 35 \cos^2 \theta) l^2 \right] \sin \theta \cos \theta = a_{12}^0,$$

$$\Omega_{zz}^0 = -\rho \left[ \mu + 2\pi\rho_1 A_2 + \frac{3}{2}\mu A + \frac{\mu}{2} (1 + 5 \cos^2 \theta) l^2 \right] = a_{33}^0,$$

$$\Omega_{yz}^0 = 0 \text{ and } \Omega_{xz}^0 = 0.$$

The corresponding variational equations are

$$\ddot{\xi} - 2\omega\dot{\eta} = a_{11}^0\xi + a_{12}^0\eta, \quad (13a)$$

$$\dot{\eta} + 2\omega\dot{\xi} = a_{12}^0\xi + a_{22}^0\eta, \quad (13b)$$

$$\ddot{\zeta} = a_{33}^0\zeta. \quad (13c)$$

Equation (13c) shows that the motion of  $m_3$  parallel to  $z$ -axis is always stable since  $a_{33}^0$  is always negative for all values of the parameters involved. The characteristic equation corresponding to the Equations (13a) and (13b) is

$$\lambda^4 - v_1^0\lambda^2 + v_2^0 = 0,$$

where  $v_1^0 = a_{11}^0 + a_{22}^0 - 4\omega^2$  and  $v_2^0 = a_{11}^0 a_{22}^0 - (a_{12}^0)^2$ . The non-collinear equilibrium points are unstable since  $v_2^0 < 0$ .

## 5. Applications

In the solar system many celestial bodies are not perfect spheres, they are either oblate or triaxial. Also, many of them are elongated in shape like asteroids. In this regard, the present model is applied to study the motion of submarine having some finite density  $\rho_3$  in the Earth-asteroid system. We consider the Earth-asteroid-submarine system. The bigger and smaller primaries are considered as Earth and asteroids respectively. Two asteroids, 216 Kleopatra and 22 Kalliope, are considered. The minimum orbit intersection distance (MOID) is taken as the distance between the primaries. The physical data for these systems is taken from Kaur and Aggarwal (2013b), Lang (1992), NASA database (<https://ssd.jpl.nasa.gov/sbdb.cgi>) and Wikipedia which is given as follows:

### 1. Earth-216 Kleopatra system

Mass of the Earth ( $m_1$ ) =  $5.97237 \times 10^{24}$  kg, equatorial radius of the Earth ( $a_1$ ) = 6378 km, polar radius of the Earth ( $a_2$ ) = 6356 km,  $\rho_1 = 1027$  kg/m<sup>3</sup>,  $\rho_3 = 1100$  kg/m<sup>3</sup>, mass of the 216 Kleopatra ( $m_2$ ) =  $4.66 \times 10^{18}$  kg, distance of 216 Kleopatra from the Earth = 1.486 A.U.

= 222302436 km, and length of the 216 Kleopatra ( $2l$ ) = 276 km.

**In dimensionless system**

$m_1 + m_2 = 1$  unit, that is  $5.97237 \times 10^{24}$  kg = 1 unit.

Thus,

$$\mu = \frac{m_2}{m_1 + m_2} = 7.80259 \times 10^{-7}.$$

Also, distance between the primaries = 1 unit, that is 222302436 km = 1 unit, therefore  $l = 6.20776 \times 10^{-7}$ ,  $A = 1.13378 \times 10^{-12}$ ,  $a_1 = 0.0000286906$ ,  $a_2 = 0.0000285917$ ,  $\rho_1 = 1.8891 \times 10^{12}$ ,  $\rho_3 = 2.02338 \times 10^{12}$ ,  $\rho = 0.0663642$ ,  $A_1 = 0.66574539$ .

**2. Earth-22 Kalliope system**

Mass of the 22 Kalliope ( $m_2$ ) =  $8.42 \times 10^{18}$  kg, distance of 22 Kalliope from the Earth = 1.638 A.U.= 245041312 km, length of the 22 Kalliope ( $2l$ ) = 215 km.

**In dimensionless system**

$\mu = 1.40982 \times 10^{-6}$ ,  $l = 4.38702 \times 10^{-7}$ ,  $A = 9.33123 \times 10^{-13}$ ,  $a_1 = 0.0000260283$ ,  $a_2 = 0.0000259385$ ,  $\rho_1 = 2.53012 \times 10^{12}$ ,  $\rho_3 = 2.70996 \times 10^{12}$ ,  $\rho = 0.0663626$ ,  $A_1 = 0.665744598$ .

**Table 4.** The locations of  $L_1$  and  $L_2$  for the Earth-216 Kleopatra and Earth-22 Kalliope system

system	$L_1(p_1, 0, 0)$	$L_2(x_1 + p_2, 0, 0)$
Earth-216 Kleopatra	$(-1.67925 \times 10^{-31}, 0, 0)$	$(0.999387, 0, 0)$
Earth-22 Kalliope	$(-1.86451 \times 10^{-31}, 0, 0)$	$(0.999736, 0, 0)$

For Earth-216 Kleopatra and Earth-22 Kalliope system, the locations of the collinear equilibrium points  $L_1$  and  $L_2$  are given in Table 4. It has been observed that for both the systems, the equilibrium point  $L_1$  collinear with the centers of the primaries exists. However, the condition  $|x_1| < a_1$  is not satisfied, therefore,  $L_2$  does not exist. Also, both the systems do not possess the non-collinear equilibrium points since  $2\pi\rho_1A_1 = (1 - \mu)(1 + l^2 + 3/2A)$  is not satisfied.

**6. Discussion**

We studied the original Robe's problem in which the structures of the bigger and smaller primaries are assumed to be hydrostatic equilibrium figure as an oblate spheroid filled with a homogeneous incompressible fluid of density  $\rho_1$  and finite straight segment respectively. Due to the presence of oblateness and length parameters, our equations of motion (1a)-(1c) are different from as those of equations obtained in Robe (1977) and analogous with as that of Hallan and Mangang (2007) if the effect of the finite straight segment is neglected. The equations of motion in Kumar et al. (2019) can be attained from our equations of motion by taking  $m_1$  as a rigid spherical shell filled with homogenous incompressible fluid instead of oblate spheroid and shifting the center of  $m_1$  from  $(0, 0, 0)$  to  $(-\mu, 0, 0)$ .

In this note we have examined the motion of infinitesimal mass  $m_3$  of density  $\rho_3$  moving inside  $m_1$ .

The equations of motion of  $m_3$  are derived under the influence of attraction of  $m_2$ , the gravitational force exerted by the fluid of density  $\rho_1$  and the full buoyancy force of the fluid  $\rho_1$ . The main aim of this work was to examine the effects of oblateness parameter  $A$  of  $m_1$  and length parameter  $l$  of  $m_2$  on the positions and stability of the equilibrium points.

We have discussed the case of unequal densities, that is when  $\rho_1 \neq \rho_3$ , since in practice it is very hard to see the case when both the densities are equal. When  $A \neq 0$  and  $l \neq 0$ , we found two collinear equilibrium points  $L_1(p_1, 0, 0)$  and  $L_2(x', 0, 0)$ . The existence of  $L_2$  depends on the conditions  $1 - 2\pi\rho_1 A_1 + \frac{3}{4}\mu < 0$  and  $|x_1| < a_1$ . The position of first collinear equilibrium point  $L_1$  does not depend on the length parameter of  $m_2$ , but influenced by oblateness  $A$  of  $m_1$ . These effects on the positions of  $L_1$  and  $L_2$  are observed in Tables 1 and 2, and shown in Figures 2 and 3 respectively. In Table 3, the effect of mass parameter  $\mu$  is numerically evaluated and the corresponding equilibrium points are plotted in Figure 4. Infinite number of non collinear equilibrium points lying on the circle given by Equation (8) are also found provided  $2\pi\rho_1 A_1 = (1 - \mu) \left(1 + l^2 + \frac{3}{2}A\right)$ . The another type of equilibrium points which lie on  $xz$ -plane are out-of-plane equilibrium points. Due to the impossibility of  $2\pi\rho_1 A_2 + \frac{2\mu(r_1+r_2)}{r_1 r_2 [(r_1+r_2)^2 - 4l^2]} = 0$ , the out-of-plane equilibrium points do not exist in the present problem.

To study the linear stability of the equilibrium points, some displacement to the positions of the infinitesimal mass have been imposed along the  $ox$  and  $oy$  axes. The equilibrium point is stable if the infinitesimal mass oscillates around it and unstable if its motion is a rapid departure from its vicinity. Using this notion of stability some conclusions were drawn for the equilibrium points in the case when  $A \neq 0$  and  $l \neq 0$ . The collinear equilibrium point  $L_1$  is stable if  $p_1 < 0$ , conditionally stable for  $0 < p_1 < A/2$  and unstable if  $0 < A/2 < p_1$ . The other collinear equilibrium point  $L_2$  is stable if  $x' < 0$ , and for  $x' > 0$  if  $v'_1 < 0$  and  $v'_2 > 0$ , then  $L_2$  is stable. Non-collinear equilibrium points are always unstable for all values of the parameters involved.

Further, we have considered two practical models namely Earth-216 Kleopatra-submarine and Earth-22 Kalliope-submarine systems. For these two presented systems, only one collinear equilibrium point  $L_1$  exist, whereas the collinear equilibrium point  $L_2$  and non-collinear points do not exist, since they do not satisfy the conditions of their existence.

## 7. Conclusion

The present study holds the Robe's restricted three-body problem with a bigger primary as an oblate spheroid which is filled with a homogeneous incompressible fluid. The smaller primary takes the shape of a finite straight segment that describes a circular motion around the bigger primary. This investigation considers the combined effects of oblateness and length of the primary bodies on the motion of an infinitesimal body, that moves inside the bigger primary. The locations of the equilibrium points are calculated. Due to the involvement of the parameters in the problem, it is observed that the motion of the infinitesimal body is possible in the plane of motion of the primaries. The present model holds two collinear equilibrium points that lie on the line segment joining the centers of the primaries. The non-collinear equilibrium points are found to lie on a circle

and are infinite in number. The problem does not possess any out-of-plane equilibrium point. The linear stability analysis is carried out and depending on the characteristic equation corresponding to the variational equations, it is obtained that the collinear equilibrium points can be stable under certain conditions, however the non-collinear are always unstable for any choice of the parameters.

## REFERENCES

- Aggarwal, R. and Kaur, B. (2014). Robe's restricted problem of 2+2 bodies with one of the primaries an oblate body, *Astrophys. Space Sci.*, Vol. 352, pp. 467–479.
- Ansari, A.A., Singh, J., Alhussain, Z.A. and Belmabrouk, H. (2019). Effect of oblateness and viscous force in the Robe's circular restricted three-body problem, *New Astronomy*, Vol. 73, 101280.
- Brouwer, D. and Clemence, G.M. (1961). *Methods of Celestial Mechanics*, Academic Press, New York.
- Chandrashekhar, S. (1987). *Ellipsoidal Figures of Equilibrium*, Dover Publications Inc., New York.
- Chauhan, S., Kumar, D. and Kaur, B. (2018). Restricted three-body problem under the effect of albedo when smaller primary is a finite straight segment, *Appl. and Appl. Math.: An Int. J. (AAM)*, Vol. 13, No. 2, pp. 1200–1215.
- Hallan, P.P. and Rana, N. (2001). The existence and stability of equilibrium points in the Robe's restricted three-body problem, *Celes. Mech. Dyn. Astron.*, Vol. 79, No. 2, pp. 145–155.
- Hallan, P.P. and Mangang, K.B. (2007). Existence and linear stability of equilibrium points in the Robe's restricted three-body problem when the first primary is an oblate spheroid, *Planetary and Space Sci.*, Vol. 55, pp. 512–516.
- Jain, R. and Sinha, D. (2014a). Non-linear stability of  $L_4$  in the restricted problem when the primaries are finite straight segments under resonances, *Astrophys. Space Sci.*, Vol. 353, pp. 73–88.
- Jain, R. and Sinha, D. (2014b). Stability and regions of motion in the restricted three-body problem when both the primaries are finite straight segments, *Astrophys. Space Sci.*, Vol. 351, pp. 87–100.
- Kaur, B. and Aggarwal, R. (2012). Robe's Problem: Its extension to 2+2 bodies, *Astrophys. Space Sci.*, Vol. 339, pp. 283–294.
- Kaur, B. and Aggarwal, R. (2013a). Robe's restricted problem of 2+2 bodies when the bigger primary is a Roche ellipsoid, *Acta Astronautica*, Vol. 89, pp. 31–37.
- Kaur, B. and Aggarwal, R. (2013b). Robe's restricted problem of 2+2 bodies when the bigger primary is a Roche ellipsoid and the smaller primary is an oblate body, *Astrophys. Space Sci.*, Vol. 349, pp. 57–69.
- Kaur, B., Kumar, D. and Chauhan, S. (2020a). A study of small perturbations in the Coriolis and centrifugal forces in RR3BP with finite straight segment, *Appl. and Appl. Math.: An Int. J. (AAM)*, Vol. 15, No. 1, pp. 77–93.
- Kaur, B., Kumar, S., Chauhan, S. and Kumar, D. (2020b). Stability analysis of circular Robe's R3BP with finite straight segment and viscosity, *Appl. and Appl. Math.: An Int. J. (AAM)*, Vol. 15, No. 2, pp. 1072–1090.

- Kumar, D., Kaur, B., Chauhan, S. and Kumar, V. (2019). Robe's restricted three-body problem when one of the primaries is a finite straight segment, *Int. J. of Non-Linear Mech.*, Vol. 109, pp. 182–188.
- Lang, K.R. (1992). *Astrophysical Data: Planets and Stars*, Springer, New York.
- Plastino, A.R. and Plastino, A. (1995) Robe's restricted three-body problem revisited, *Celes. Mech. Dyn. Astron.*, Vol. 61, pp. 197–206.
- Riaguas, A., Elipe, A. and Lopez-Moratalla, T. (2001). Non-linear stability of the equilibria in the gravity field of a finite straight segment, *Celes. Mech. Dyn. Astron.*, Vol. 81, pp. 235–248.
- Robe, H.A.G. (1977). A new kind of three-body problem, *Celes. Mech. Dyn. Astron.*, Vol. 16, pp. 343–351.
- Sharma, R.K. and Subbarao, P.V. (1976). Stationary solutions and their characteristic exponents in the restricted three-body problem when the more massive primary is an oblate spheroid, *Celes. Mech. Dyn. Astron.*, Vol. 13, pp. 137–149.
- Shrivastava, A.K. and Garain, D. (1991). Effect of perturbation on the location of libration point in the Robe restricted problem of three bodies, *Celes. Mech. Dyn. Astron.*, Vol. 51, pp. 67–73.
- Singh, J. and Mohammed, H.L. (2012). Robe's circular restricted three-body problem under oblate and triaxial primaries, *Earth, Moon, and Planets*, Vol. 109, pp. 1–11.
- Singh, J. and Mohammed, H.L. (2013). Out-of-plane equilibrium points and their stability in the Robe's problem with oblateness and triaxiality, *Astrophys. Space Sci.*, Vol. 345, pp. 265–271.
- Singh, J. and Sandah, A.U. (2012). Existence and linear stability of equilibrium points in the Robe's restricted three-body problem with oblateness, *Advances in Mathematical Physics*, 18 pages.
- Wang, X., Wu, N., Zhou, L. and Xu, B. (2018). On existence of out-of-plane equilibrium points in restricted three-body problem with oblateness, *Earth and Planetary Astrophysics*, 11 pages.